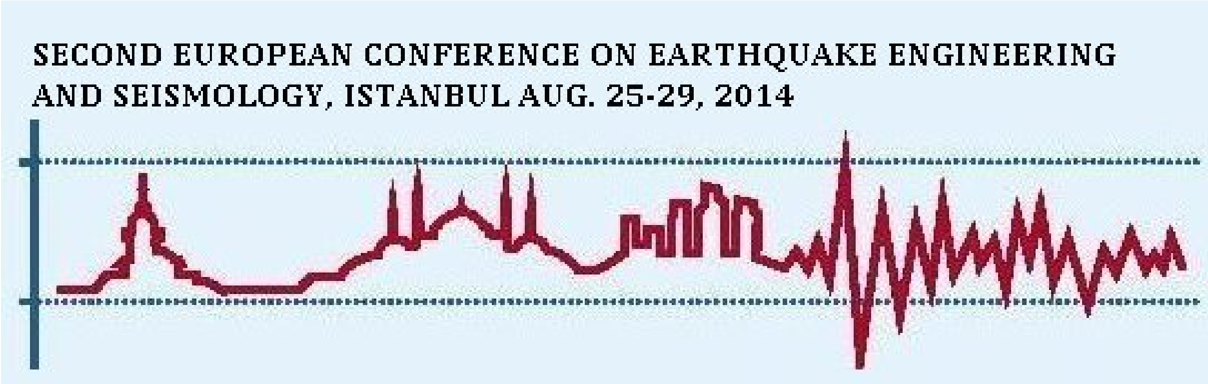

T-H DYNAMIC AND NONLINEAR STATIC ANALYSIS FOR THE PV CANOPY OF THE NEW ATHENS OPERA HOUSE

Gregory Penelis[1], George Penelis[2], Kostas Paschalidis[3], Vasileios Papanikolaou[4] and Elias Paraskevopoulos[5]

ABSTRACT

The Athens Opera House is a R/C building part of the Stavros Niarchos Cultural Center (SNFCC), a project designed by Renzo Piano, currently being constructed with a budget of 500 Million Euro. The ferrocement canopy of the Opera Building is made up of two ferrocement skins: the superior one (top skin) and the inferior one (bottom skin); they are connected together by Ferrocement diaphragms and diagonal steel circular hollow tube sections. The current paper outlines the analytical approaches utilised during the implementation design and correlates these to the experimental work that took place. The initial design has been executed by Expedition Engineering, London.

INTRODUCTION

The Athens Opera House is a seismically isolated building using a number of inverted pendulum seismic isolators. This reduces the horizontal inertial forces transmitted to the superstructure for excitations of over 5.5%g. This has allowed the R/C building to be detailed as DCL with a q=1.50.
The canopy that is based on the roof of the Opera building is foreseen as the most impressive architectural feature of the whole complex and since its inception it aimed towards an innovative and challenging design. A general section of this Canopy and the Opera house is shown in figure 1. It was decided that the canopy will be a composite ferrocement-steel structure with the following distinct features:

- The structural system resembles that of a space truss
- The top and bottom cords of the space truss are of ferrocement skin
- The top and bottom skin have double curvature
- The ferrocement skins are ribbed membranes

GEOMETRY

The canopy is 100mx100m in plan and 4.4m height at midspan. It rests upon 30 columns which result in a clear span of 75m in the long direction and 50m in the short dimension (figure 2).

[1] Dr, Civil Engineering, Penelis Consulting Engineers SA, Thessaloniki, penelis@penelis.com
[2] Em. Professor, AUTH, Thessaloniki, gpenelis@civil.auth.gr
[3] Dr, Civil Engineering, Penelis Consulting Engineers SA, Thessaloniki, kp@penelis.com
[4] Lecturer, AUTH, Thessaloniki, billy@civil.auth.gr
[5] Dr, Civil Engineering, Penelis Consulting Engineers SA, Thessaloniki, penelis@penelis.com

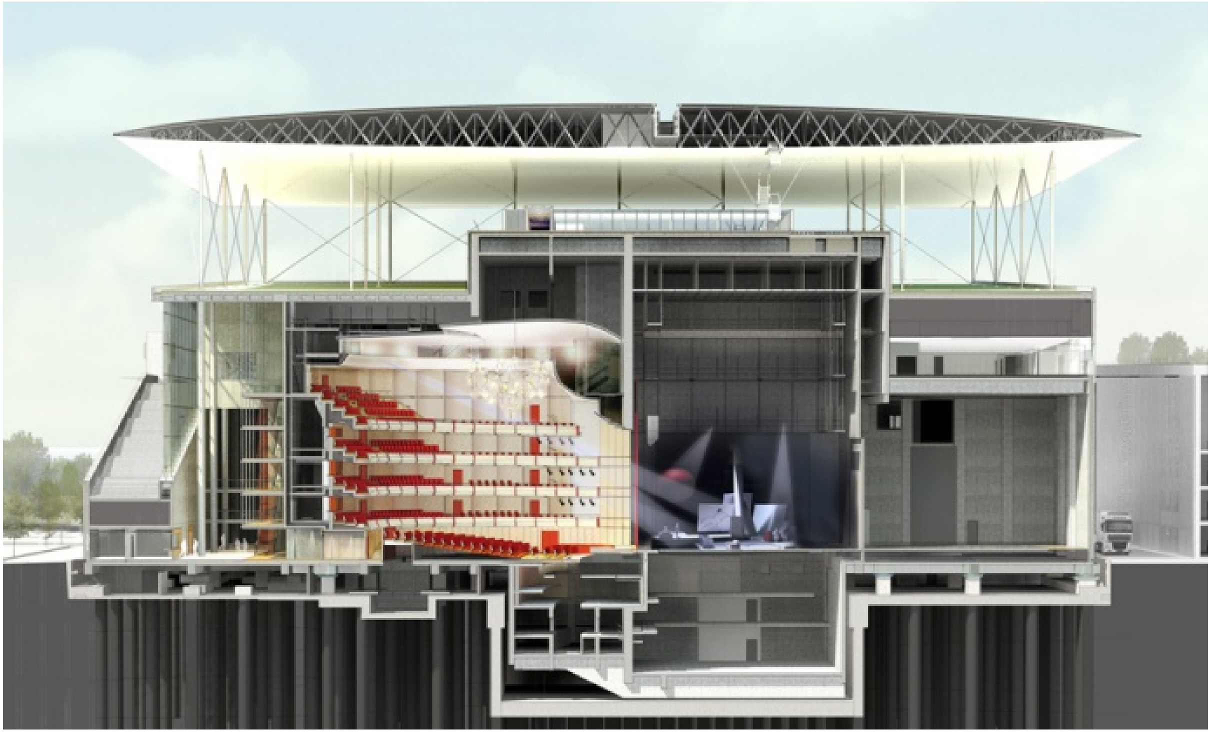

Figure 1. Cross Section of the Opera House and the Canopy on top of it

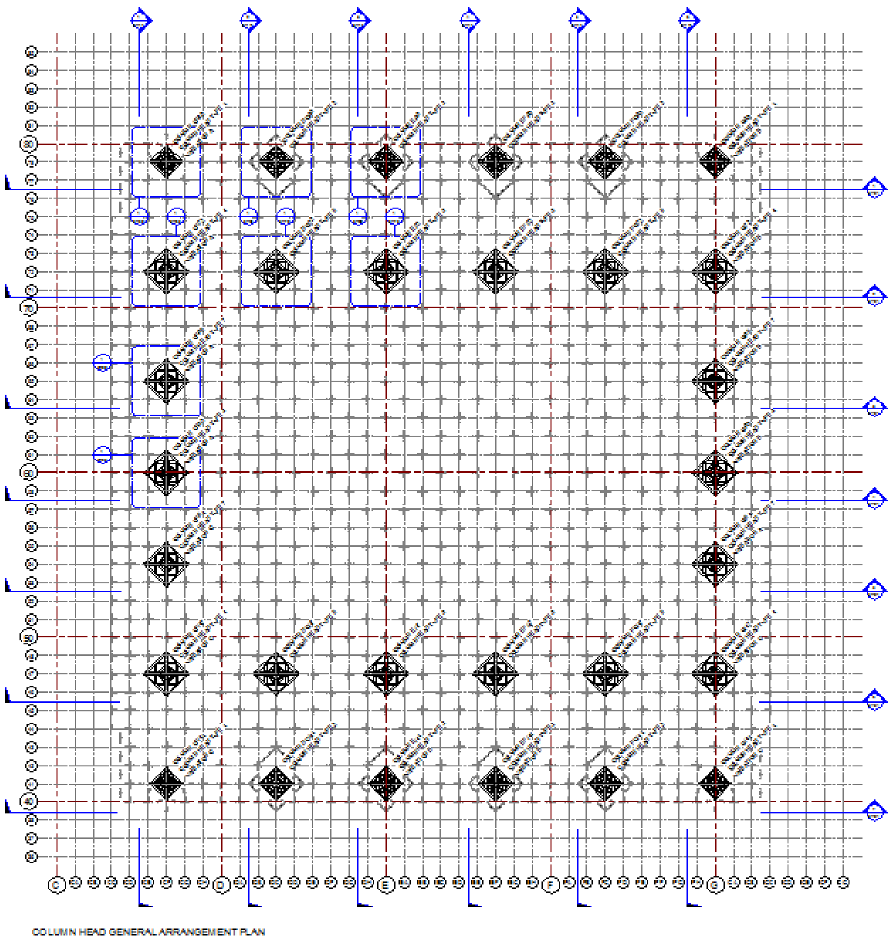

Figure 2. Plan view of the canopy support columns

The canopy rests upon the Opera building using 30 CHS (Tubo) columns. The connection between the CHS columns and the canopy is through a column head, an assembly of spring and dampers that essentially hangs the canopy from the columns (fig.4).

FERROCEMENT SECTIONS

The bottom and top skin of the canopy are composed of double curvature ferrocement skins. The material properties of the ferrocement mortar are shown in table 1

Table 1. Ferrocement mortar properties

SAMPLES	PROPERTY	MIX DESIGN #1 Superfluid	MIX DESIGN #2 Low Workability
Cubes 100x100x100	Compressive strength (7 days)	64 MPa	64 MPa
	Compressive strength (28 days)	90 MPa	88 MPa
	Shrinkage (28 days)	0.390 mm/m	0.390 mm/m
Cylinders 150x300	Compressive strength (7 days)	56 MPa	56 MPa
	Compressive strength (28 days)	80 MPa	80 MPa
	Elastic modulus	33 GPa	33 GPa
	Density of hardened mortar	< 2290 kg/m^3	< 2290 kg/m^3

The meshes used for reinforcement are the following:

- Mesh type 1: Ø1.0mm, grid 10x10mm^2, B430A
- Mesh type 2: Ø1.6mm, grid 12.5x12.5 mm^2, B500A
- Mesh type 3: Ø2.5mm, grid 25x25 mm^2, B500A
- Mesh type 4: Ø5.0mm, grid 50x50 mm^2, B500A
- Mesh type 5: Ø10.0mm, grid 50x50 mm^2, B500C

The meshes are arranged in a sandwich pattern in order to create a heavily reinforced ferrocement section (3-6%). The main concept is that the external meshes are thin to provide crack control and durability while the internal are thicker.

Both the bottom and top skin are ribbed with ribs every 62cm in order to provide bending stiffness, and all the ribs all have rebars B500C as longitudinal reinforcement. An indicative T section of ferrocement is shown in figure 3.

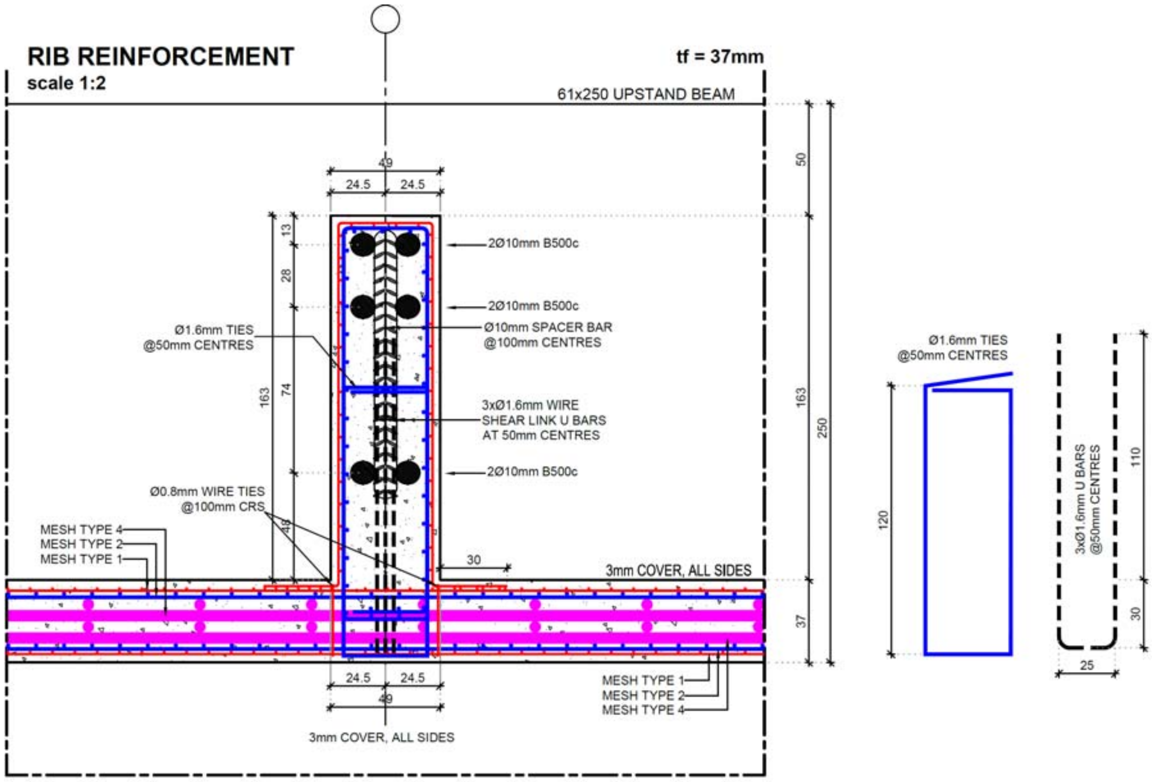

Figure 3. 3D Indicative T section of ferrocement for the bottom skin

COLUMN HEADS

As mentioned the vertical dynamic behaviour is controlled by a set of springs and dampers. To that effect each column has on top of it a column head that consists of 4 inclined springs, 2 inclined dampers and friction vertical pads as shown in figure 4:

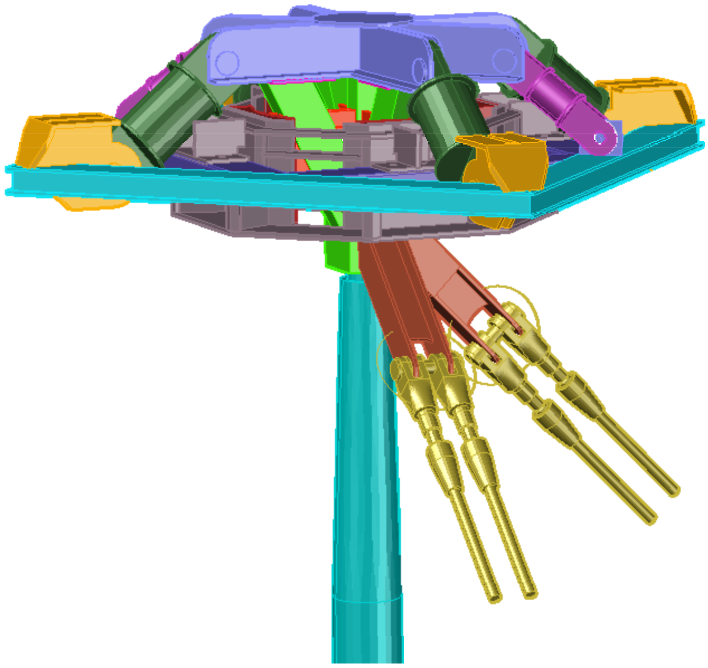

Figure 4. 3D BIM modelling of the Column head asembly

The four inclined springs are the load path for all vertical loads (gravity, wind and seismic excitation), while the two inclined dampers provide the required energy dissipation so that the canopy does not resonate to wind loading. The vertical friction pads are created from Mageba roboslide material (often used for inverted friction pendulum seismic isolators) and aim to limit the wind vibration for a low wind loading of approximately 12.5% of the design wind.

ELASTIC DYNAMIC ANALYSIS

As has already been mentioned the canopy rests upon the Opera building using 30xCHS steel columns via an elastic spring/ viscous plastic dampers assembly. In order to model the global behaviour and the interaction between the opera and the canopy an accurate F.E. modelling representation was elaborated using the Scia Engineer software code (figure 5).
The analysis was elastic dynamic analysis using the horizontal seismic excitation of 5.5%g (the threshold of the seismic isolation) and the EN1998 site specific spectrum for the vertical excitation.
The wind loads were applied as static loads using extensive wind tunnel testing executed during the preliminary design phase at CTSB.
As expected the critical loading for the canopy and the CHS columns are the ULS wind combinations.

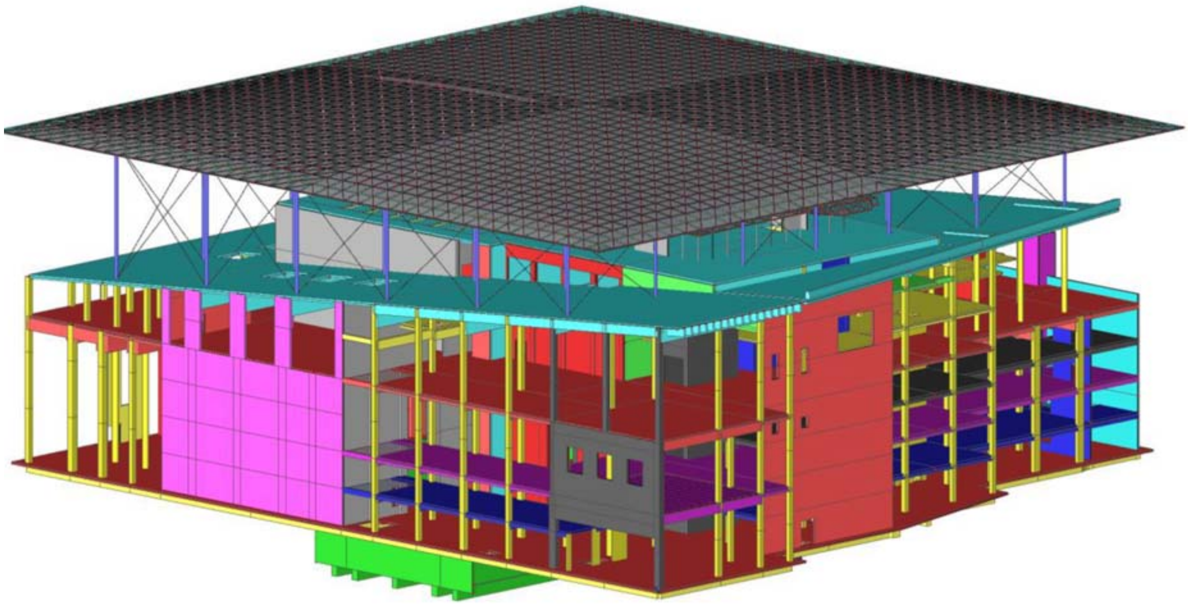

Figure 5. 3D structural modelling in Scia Engineer

T-h NL DYNAMIC ANALYSIS

Taking into account that the wind load combinations are the most critical behaviour the dynamic response of the canopy was investigated using t-h nonlinear analysis. For the sake of simplicity the canopy has been modelled as flat surface with shell elements in Etabs2013 (fig. 6). The stiffness and mass distribution of these have been selected the same as the full canopy model as is evident from table 2 showing the Eigen periods of the two models. The model has been created from the steel columns upward, i.e. excluding the opera model. This has been obviously selected in order to facilitate the t-h NL analyses.

Table 2. Dynamic Characteristics of accurate and approximate modelling

	Accurate Canopy model							Simplified Canopy Model					
Mode	Period	UX	UY	UZ	RX	RY	RZ	**Period**	**UX**	**UY**	**UZ**	**RX**	**RY**	**RZ**
1.000	0.774	0.019	92.645	0.009	39.211	0.027	4.618	0.800567	0.000	0.959	0.000	0.000	0.000	0.041
2.000	0.761	21.544	0.016	1.355	0.017	60.829	0.000	0.750004	0.998	0.000	0.000	0.000	0.002	0.000
3.000	0.744	1.889	0.021	89.156	0.005	2.465	0.002	0.732801	0.000	0.000	0.920	0.000	0.000	0.000
4.000	0.717	76.383	0.005	0.827	0.002	36.230	0.001	0.715699	0.002	0.000	0.000	0.000	0.996	0.000
5.000	0.663	0.000	2.052	0.035	54.942	0.000	0.427	0.630459	0.000	0.000	0.000	0.992	0.000	0.000
6.000	0.637	0.003	0.139	0.004	0.068	0.001	0.011	0.57151	0.000	0.000	0.000	0.000	0.000	0.000
7.000	0.553	0.001	0.005	2.127	0.001	0.001	0.093	0.546235	0.000	0.041	0.000	0.000	0.000	0.959
8.000	0.535	0.002	5.082	0.000	0.864	0.001	94.807	0.528112	0.000	0.000	0.016	0.000	0.000	0.000
9.000	0.499	0.048	0.001	3.872	0.000	0.022	0.010	0.482526	0.000	0.000	0.062	0.000	0.000	0.000
10.000	0.456	0.090	0.006	0.223	0.002	0.053	0.011	0.35512	0.000	0.000	0.000	0.000	0.001	0.000
11.000	0.441	0.000	0.004	0.001	3.353	0.000	0.011	0.355098	0.000	0.000	0.000	0.008	0.000	0.000
12.000	0.327	0.000	0.011	0.006	0.001	0.002	0.000	0.233201	0.000	0.000	0.000	0.000	0.001	0.000

The four inclined springs of the column heads have been modelled as one nonlinear LINK element with a vertical stiffness corresponding to the combined behaviour of 4 springs. The main issue is the large displacements geometric nonlinearity as we have elements of 50-100cm lengths which move a distance of 25cm in total. This vertical displacement causes a change in the stiffness of the effective vertical spring. This issue was tackled using a multilinear elastic spring property as shown in figure 7.

The 2 inclined dampers have been modelled as one Nonlinear damper LINK element with a vertical damping coefficient corresponding to the combined behaviour of 2 dampers C=150 kN(sec/m)$^{0.15}$.

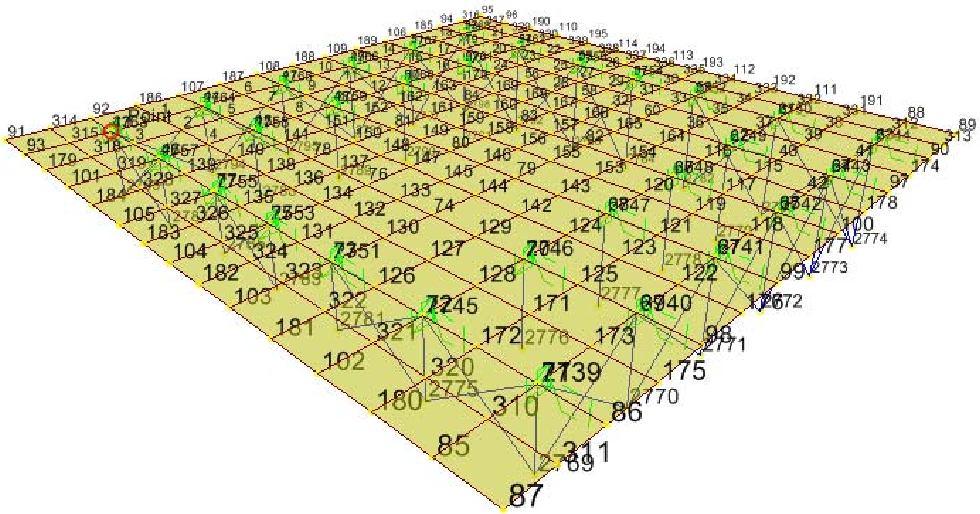

Figure 6. Simplified 3D structural modelling in Etabs 2013

The friction pads have been modelled as a single friction pendulum element placed horizontally taking into account that it is from roboslide sliding material. The element is a single node Nlink element.
The actual situation as it is well known, has 8 individual pads placed at pairs (up and down) at each side of the two directions xx, yy. Per direction only 2 pads are always active as following:

- In case of wind shear only the two pads of the same direction that are in compression are active.
- In case of local bending or global canopy overturning, in each direction two opposite pads are active (top one side bottom at the other side).

The axial forces from these conditions have been defined in order to simulate one single rubber isolator with rigid plastic behaviour and a yield force that corresponds to the friction capacity of 2 active pads per direction as following:

- In result there are 2 friction pad arrangements, one with a lever of 33cm (short heads, axes 41 & 78), and one with a lever of 64cm (tall heads).

- The average rotations of the canopy at the location of the column heads were calculated from the precise model for G. The averaging was done separately for the 2 friction pad arrangements.
- Those rotations were multiplied with the steel column stiffness 4EJ/L and the resulting moments were divided by the lever (33cm or 64cm) to produce the forces acting on the pads. These forces are approximately a quarter of the column head design forces.
- Those forces are multiplied by the friction coefficient μ=0.04 (roughly the same with the base isolators) and the resulting shear force was assigned as the yield strength of an elastic-perfectly plastic nonlinear element.
- 30 such single-node elements were assigned to the model.

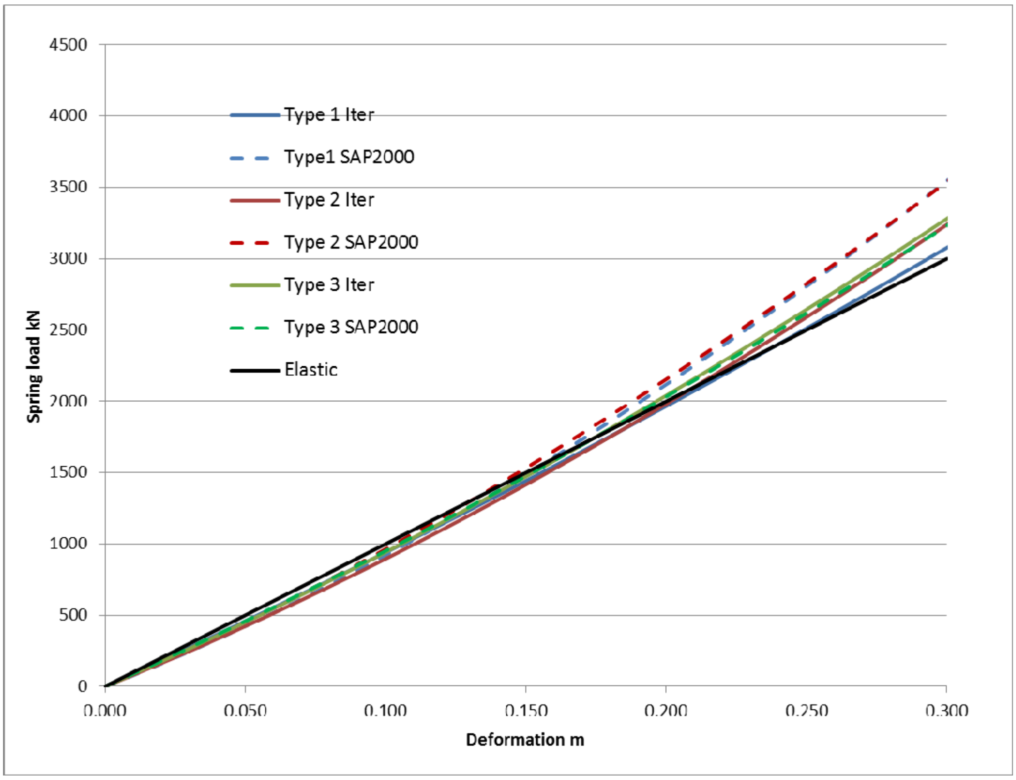

Figure 7. Multilinear elastic springs to account for geometric nonlinearity of inclined springs

The T-h nonlinear analysis has been performed for wind and earthquake excitations to assess the effect of the following factors:

- Spring hooks constants
- Dampers coefficients
- Application of the friction pads
- Estimation of the dynamic amplification factors from these parameters and comparison to the elastic design of the ferrocement, steel connections and column heads already executed by the ER design.
- Life cycle and total travel distance of the system

The following excitations were applied, following the static loads, for the case of seismic loading:

- An EC8 compatible artificial accelerogram (figure 8)
- The 14/08/2003 Lefkada event Mw= 6.3
- The 09/09/1999 Athens event (Kede station) Mw=5.9

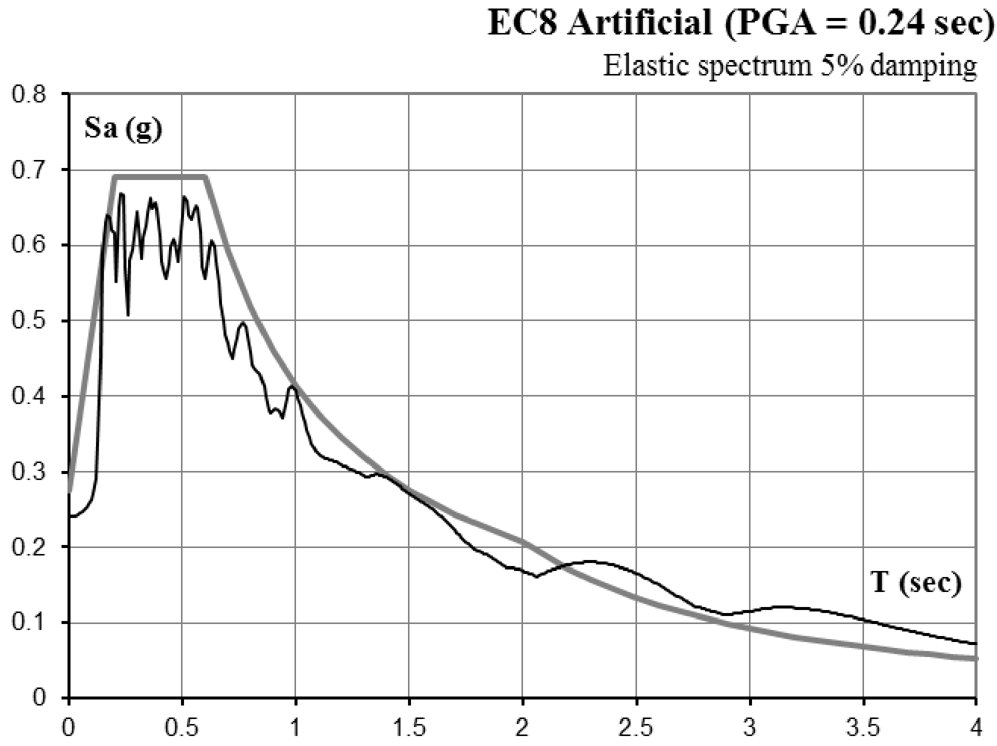

Figure 8. Artificial accelerogram Spectra Vs EN1998 spectra

For the wind dynamic excitation the fact that the downward and upward wind loads are uneven lead to the development of a custom uneven sinusoid function as shown in figure 9.
The design wind for V_{mean}=37m/sec has a period of excitation 1.33sec, defined as per EN1991-4 §E1.3.1 using the following equation:

$$n=(V_{mean}\cdot St)/b$$

where

- b: is the reference width of the cross section at which resonant vortex sheding occurs (up and down) and where the modal deflection is maximum for the structure (canopy) =4.50m
- V_{mean} is the mean value of the wind loading causing the cross wind vibration =37.50m/sec
- St: is Strouhal number as defined in E.1.3.2 (EN1991-Annex E) = 0.09

Having in mind that the predominant period of vibration of the canopy is equal to T=0.73sec it is concluded that the frequency of excitation of T=1.33sec is out of phase with the structure and does not create a resonance problem.
However as an absolute extreme the effects of a wind with frequency of excitation T=0.73sec was also investigated, although it correspond to a wind speed higher than the 100 years wind (figure 9).

Using the above, the total vertical distance travelled in 50 years is calculated taking into account the cumulative ΔS/S of the EN1991-4 Annex B relation of figure B3. This results a total distance of 110 km for 50 years or 55km for 25 years of the moving parts required life time. The springs dampers and friction pads parts have actually been prescribed with a warranty of 255km of vertical movement.

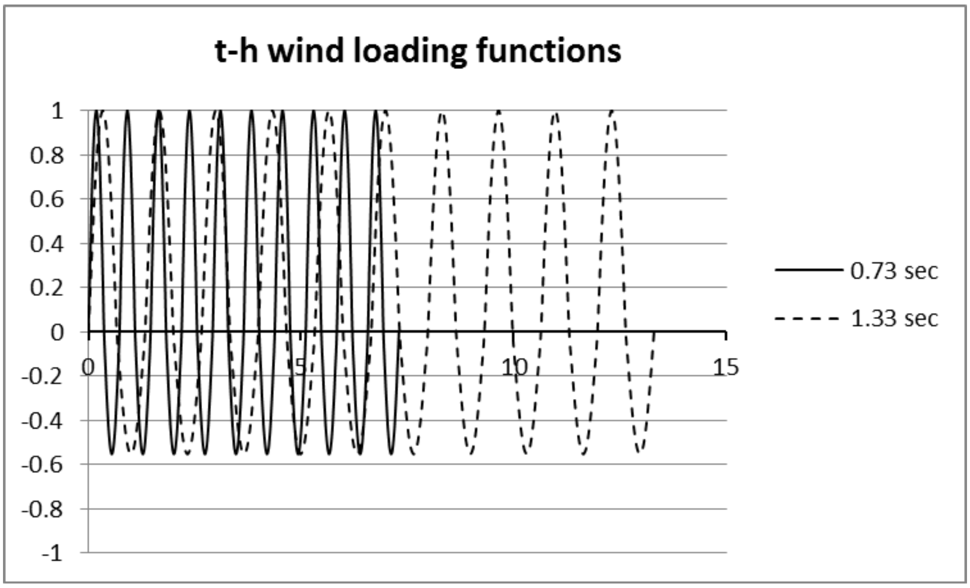

Figure 9. T-h custom functions for design wind (1.33s) and resonant wind (0.73s)

The response for the design wind gust as well as the effect of resonance (wind with the same predominant period as the canopy) is shown in figure 10. These collaborate the maximum deformations predicted using the elastic analysis approach.

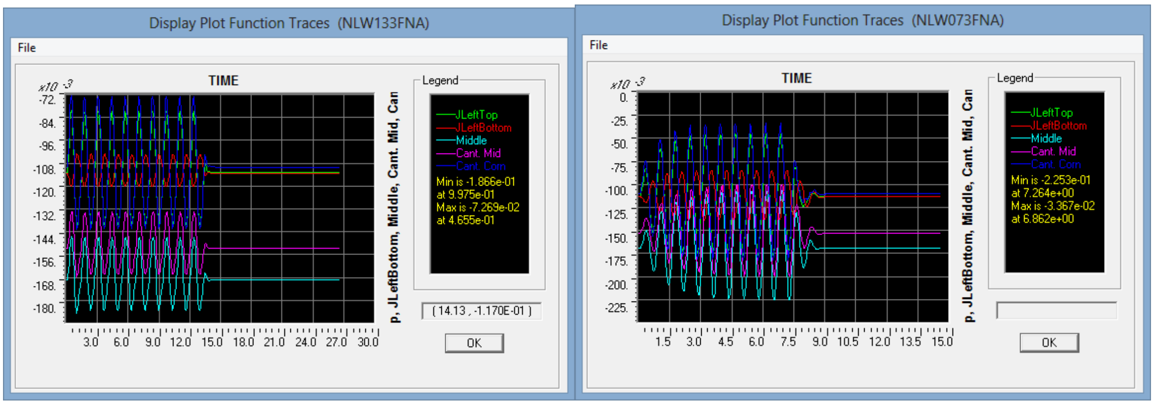

Figure 10. Design wind response (left); Resonance wind (right)

NL STATIC ANALYSIS

Static nonlinear analysis procedure was developed in order to estimate the nonlinear performance of the canopy under vertical uniformly distributed loads, thus resulting in the available overstrength (very significant) as well as the available ductility (non-ductile structure). The loads were applied according to the self-weight distribution (elastic) and were further increased by applying a step wise multiplier (nonlinear).

The application of the analysis required the development of a custom step by step non iterative procedure for the nonlinear application of the loads, which utilised the API of SAP2000 driven by PYTHON scripts.

This procedure required the pre-determination of yield and failure criteria (M-N interaction surfaces, fig.11) for the ferrocement T sections and flanges, the post yield behaviour of ferrocement elements, the introduction of the characteristics of the low ductility thin rebar meshes (1mm-10mm diameter) etc.

The resulting ultimate capacity of the ferrocement skins of the canopy (fig.11 and fig.12) corresponds to 2.68 times the ULS design load which is much more than the most critical element of the whole structure that is the available movement capacity of the canopy (1.35xULS).

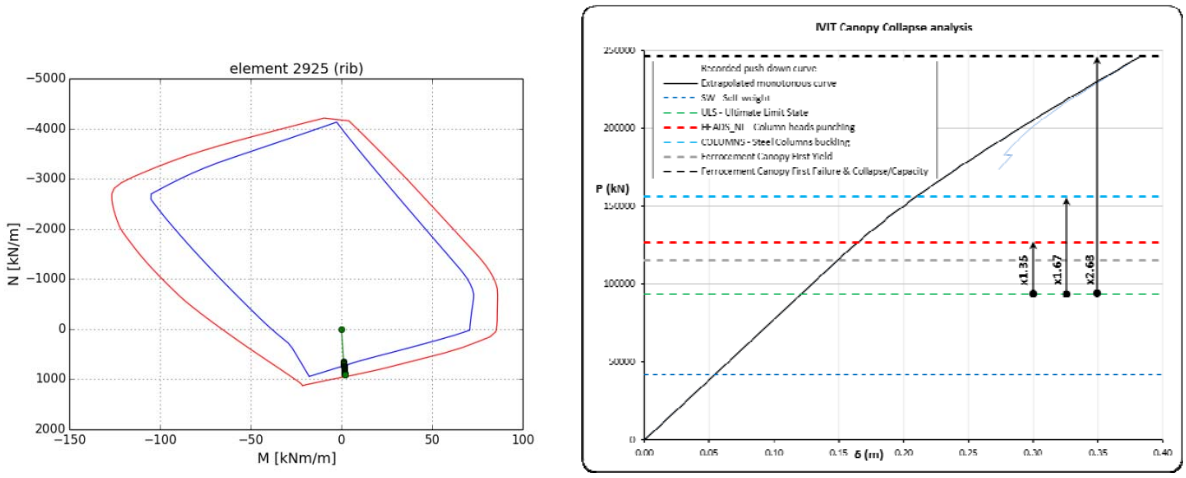

Figure 11. Section analysis of ferrocement (left) and push-down curve of canopy (right)

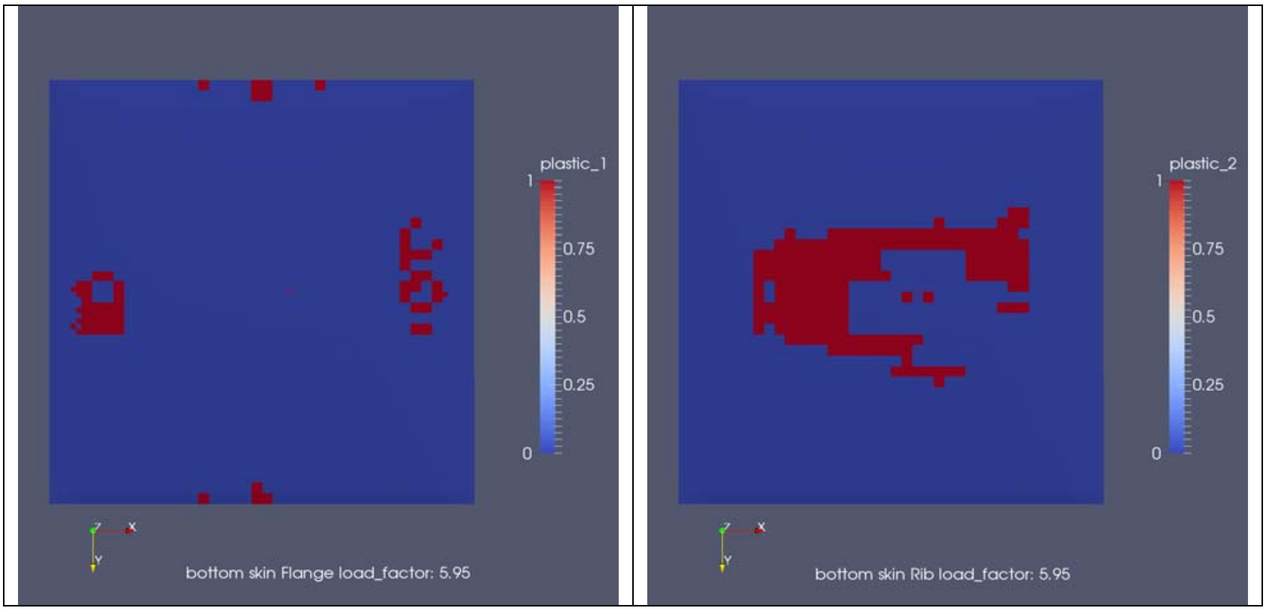

Figure 12. Bottom skin plastic elements (failure)

CONCLUSIONS

The paper attempts to demonstrate the key elements of the design process for an innovative and complex structure. All available design tools have been utilised, from elastic analysis to NL t-h and static analysis in order to verify the design. However in such complex structures analysis is not the only tool, hence a very extensive set of tests have been commissioned for the verification of critical elements of the structure such as the ferrocement sections and the column heads. These tests are indicatively shown in the following table as the presentation is not part of this paper.

Table 3. Summary Table of Experimental work

FERROCEMENT TESTS				
i	**Test**	**Samples**	**Result**	**Remarks**
1	Class A - Biaxial Compression Tests of 2.0m x 2.5m panels	6	OK	Biaxial compression of 2.0 m x 2.5 m panels reinforced with beams and ribs

2	Class B - Top & Bottom ER thickenings shear tests	13 top skin 13 bottom skin	OK	Ferrocement plates reinforced with both ribs and beams were subjected to in-plane biaxial shear at the thickenning
3	Class B – JVIT new thickenings shear tests	4	OK	Ferrocement plates reinforced with both ribs and beams were subjected to in-plane biaxial shear at the thickenning
4	Class C - Shear test of thickenings' vertical M10 anchors	4	OK	Ferrocement panels reinforced with both ribs and a beam were rigidly clamped (perfect elimination of all degrees of freedom of the panel) and pure shear loads were imposed on the two metallic threaded bars embedded in the beam of the panels.
5	Class D - Pull-out of thickenings' vertical M10 anchors	2	OK	Specimens Shaw cut from ferrocement panels were subjected to pure tensile pull-out.
6	Cold Joint separation test (rib-plate debonding)	6	OK	Strength of the bond between the rib and the plate of the specimens was tested
7	Lapping length test, Ø5 and Ø10	4+4	OK	“dogbone” specimens to subjected to direct tension to plot the respective force – displacement curve
8	T-beam 4-point test for shear capacity	3	OK	“Tau” - shaped beam specimens were subjected to four-point bending (4PB).
Column Head Tests				
1	Type 1 Column Head full test Vertical	1	N/A	A full scale test of type 1 column head executed for vertical movement (low velocity)
2	Type 4 Column Head full test Vertical	1	N/A	A full scale test of type 4 column head executed for vertical movement (low velocity)
3	Spring tests EN15129	1	N/A	ITT and Production tests
4	Damper tests EN15129	1	N/A	ITT and Production tests

REFERENCES

E.C.8-1/EN1998-1 (2004). Design of structures for earthquake resistance: General rules, seismic actions and rules for buildings, CEN, Brussels, Belgium.

EC2-1-1/EN1992-1-1 (2004). Design of concrete structures - Part 1-1: General rules and rules for buildings. CEN, Brussels, Belgium.

ECtools v1.5, ‘EN User manual’, 3Pi Software ltd, Thessaloniki, Greece, www.ectools.eu, 2014.

Etabs, Integrated Building Design Software, Computers and Structures Inc, Berkeley, California, 2013.

Papanikolaou, V. - Analysis of arbitrary composite sections in biaxial bending and axial load – Computers & Structures 98-99 (2012

Penelis, G.G. and Kappos, A.J. (1997). Earthquake-Resistant Concrete Structures. SPON E&FN (Chapman and Hall), London.

Penelis, G.Gr. and Penelis, Gr.G. (2014), Concrete Buildings in Seismic Regions, CRC Press (T&F), London

SAP2000 V-15, ‘Integrated software for structural analysis and design’, Computers and Structures, Inc.

SAP2000, Three dimensional static and dynamic finite element analysis and design of structures, Computers and Structures Inc. (1999), Berkeley, California, 1999.

Scia Engineer 2013, User Manual, Nemetschek Scia nv, Industrieweg 1007, 3540, Herk-de-Stad, Belgium, 2013.